Level-set evolution with region competition: Automatic 3-D segmentation of brain tumors

Conference Paper · February 2002

DOI: 10.1109/ICPR.2002.1044788 · Source: IEEE Xplore

3 authors, including:

Elizabeth Bullitt
University of North Carolina at Chapel Hill
107 PUBLICATIONS **4,391** CITATIONS
SEE PROFILE

Guido Gerig
NYU Tandon School of Engineering
398 PUBLICATIONS **20,947** CITATIONS
SEE PROFILE

Level-Set Evolution with Region Competition: Automatic 3-D Segmentation of Brain Tumors

[1]Sean Ho, [2]Elizabeth Bullitt, and [1,3]Guido Gerig *

[1]Department of Computer Science, [2]Department of Surgery, [3]Department of Psychiatry
University of North Carolina, Chapel Hill, NC 27599, USA
E-mail: {seanho,gerig}@cs.unc.edu

Abstract

We develop a new method for automatic segmentation of anatomical structures from volumetric medical images. Driving application is tumor segmentation from 3-D MRIs, which is known to be a very challenging problem due to the variability of tumor geometry and intensity patterns. Level-set snakes offer significant advantages over conventional statistical classification and mathematical morphology, however snakes with constant propagation need careful initialization and can leak through weak or missing boundary parts. Our region competition method overcomes these problems by modulating the propagation term with a signed local statistical force, leading to a stable solution.

A pre- vs. post-contrast difference image is used to calculate probabilities for background and tumor regions, with a mixture-modelling fit of the histogram. Preliminary results on five cases with significant shape and intensity variability demonstrate that the new method might become a powerful and efficient tool for the clinic. Validity is demonstrated by comparison with manual expert segmentation.

1. Introduction

Segmentation of volumetric image data is still a challenging problem, and successful solutions either often are based on simple intensity thresholding or by model-based deformation of templates. Classical snakes [3] have had the problem of being "only as good as their initialization", even when using level-set snakes in 3-D [7, 8, 2]. A powerful extension is obtained by combining level-set evolution with statistical shape constraints [5], but the statistical prior is not easily obtainable in some applications. Level-set evolution with fixed propagation direction must be initialized either completely inside or outside sought objects. At locations of missing or fuzzy boundaries, the constant propagation force is often strong enough to counteract global smoothness, and "leaks" through these gaps. This observation led to a new concept of region competition, where two adjacent regions compete for the common boundary [11], additionally constrained by a smoothness term.

The driving problem discussed in this paper is the segmentation of 3-D brain tumors from magnetic resonance image data. Tumors vary in shape, size, location, and internal texture, and tumor segmentation is therefore known to be a very challenging problem. Intensity thresholding followed by erosion, connectivity, and dilation is a common procedure but only applicable to a small class of tumors presenting simple shape and homogeneous interior structure. Warfield et al. [9, 10, 4] demonstrated a methodology based on elastic atlas warping for brain extraction and statistical pattern recognition for brain interior structures. The intensity feature was augmented by a "distance from the boundary" feature to account for overlapping probability density functions, and finally run through opening/closing. The method has been shown to be successful for simply-shaped tumors with homogeneous texture.

The approach presented herein aims at providing a more generic and fully automatic method for the segmentation of blobby-shaped tumor structures. We developed a robust 3-D level-set method in a region competition framework, with variable topology and smoothness constraints.

2. Tumor segmentation procedure

We start with an intensity-based fuzzy classification of voxels into tumor and background classes. The details of this initial classification are given in Section 4.2. This tumor probability map is then used to locally guide the propagation direction and speed of a level-set snake. The tumor probability map is also used to derive an automatic initialization of the snake. Image forces are balanced with global smoothness constraints to converge stably to a smooth blobby tumor segmentation of arbitrary topology.

2.1. Multiparameter image data

Our images are multichannel 3D magnetic resonance images that show different aspects of the tumor region. High-resolution T1-weighted MRIs are commonly used for detailed imaging of neuroanatomy, but by themselves do not

*Supported by NIH-NCI R01 CA67812. Partially supported by NIH-NCI P01 CA47982.

distinguish tumor tissue well. T2-weighted MRIs do highlight tumor tissue and surrounding edema, but are often difficult to obtain in high resolution. Of great use is a post-contrast T1-weighted MRI, where contrast agent has been injected into the bloodstream to highlight the tumor. In this work we use T1-weighted pre- and post-contrast 3D images.

2.2. Image forces

In a deformable model segmentation scheme, the model is driven by image forces and constrained by prior information on the shape of the model. In level-set snakes, the image forces are generally governed by the gradient magnitude, and the shape prior is a form of smoothness.

The traditional "balloon" level-set snakes use a constant propagation term, so the balloon can only grow or only shrink. Hence the snake must be initialized either completely inside or outside the tumor. Here, we locally modulate the propagation term by a signed image force factor between -1 and +1, causing the snake to shrink when outside the tumor and expand when inside the tumor.

2.3. Smoothness constraints

If the snake were only guided by image forces, it would leak into many small noisy structures in the image that are not part of the tumor. A commonly used, standard way to constrain level-set snakes is to apply mean curvature flow to the snake contour; in the level-set formalism this is easily done by adding a term to the snake evolution equation. We also apply a smoothing to the implicit function in order to aid numerical stability of the algorithm.

3. Level-set snake evolution

A classical level-set snake is defined as the zero level-set of an implicit function ϕ defined on the entire image. The evolution of the snake is defined via a partial differential equation on the implicit function ϕ.

A standard level-set snake propagates normal to its boundary uniformly at a constant speed α. Our region competition-based snake modulates this propagation term using image forces to change the direction of propagation, so that the snake shrinks when the boundary encloses parts of the background (B), and grows when the boundary is inside the tumor region (A):

$$\frac{\partial \phi}{\partial t} = \alpha(P(A) - P(B)) \left|\nabla \phi\right|$$

The image forces need to be balanced with some smoothness constraints; a standard technique is to apply mean curvature flow to the snake contour. The strength of the smoothing is controlled with a constant factor c_{MCF}.

Lastly, to help ensure numerical stability of the forward-in-time, centered-in-space solution of the partial differential equation, we apply a uniform Gaussian smoothing force on the implicit function ϕ. The MCF term applies a smoothing on the level-set contour, but does not prevent the implicit function ϕ from having sharp discontinuities. An additional constant factor c_{sm} controls the strength of this smoothing. The final equation driving the level-set evolution:

$$\begin{aligned} \frac{\partial \phi}{\partial t} &= \alpha(P(A) - P(B)) \left|\nabla \phi\right| \\ &+ c_{\mathrm{MCF}} \nabla \cdot \left(\frac{\nabla \phi}{|\nabla \phi|} \right) |\nabla \phi| \\ &+ c_{\mathrm{sm}} \nabla^2 \phi \end{aligned}$$

4. Application to tumor segmentation

4.1. MRI methods

Our image datasets are from patients with meningioma and glioblastoma brain tumors, acquired on a 1.5T clinical scanner (except for one acquired on a 3T scanner). We used pre- and post-contrast T1-weighted images of the whole head, having an in-plane resolution of 256x256 and about 120 slices (depending on the individual dataset), with a voxel resolution of $1 \times 1 \times 1.5mm^3$.

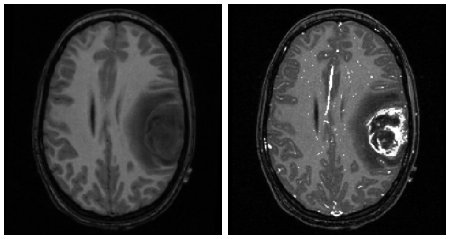

Figure 1. Axial cross-section of T1-weighted 3D MRI, without (left) and with (right) contrast agent.

4.2. Tumor probability map

Of critical importance in the formulation of the competition level-set snake is the probability map, a scalar field on the image which specifies, voxel by voxel, a probability that the given voxel belongs to the tumor or to the background. The two T1-weighted images, with and without contrast agent, are registered using MIRIT [6] and a difference image is obtained voxel-by-voxel. The histogram of this difference image (see Fig. 2) clearly shows a symmetric distribution around zero and a second distribution, strictly positive, related to regional changes caused by contrast. In this preliminary work, we fit the histogram by a mixture density of two distributions, a Gaussian to model noise around zero and a Gamma distribution to model enhancing tumor tissue. We use the NonlinearFit package provided by Mathematica. The scalar field derived from the posterior probability of enhancing tumor tissue is rescaled

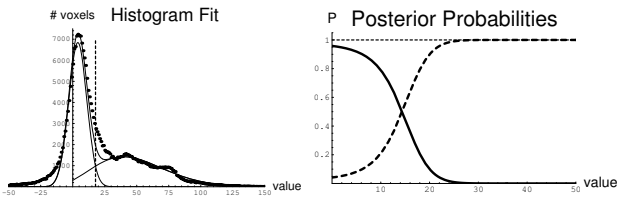

Figure 2. Left: histogram of difference image, fit with a Gaussian for background and a Gamma for tumor. Threshold is shown as a vertical line. Right: Posterior probabilities for background (solid) and tumor (dotted).

into the range $[-1, 1]$ and passed into the level-set algorithm as the probability map $P(A) - P(B)$ shown in Figure 3(a).

For computational speed, the datasets are subsequently cropped to the region around the tumor, however the algorithm works just as well on the whole brain.

The probability map from the difference image is rather noisy, and includes many regions that should not be considered part of the tumor. It is known that blood vessels and bone marrow also take up gadolinium. In addition, the ring-shaped gadolinium enhancement common in glioblastoma tumors results in misclassification of many voxels in the center of the tumor. It is clear that intensity-based tissue classification alone is insufficient for satisfactory segmentation of the tumor. The level-set snake uses this fuzzy classification heavily for its image forces, but adds needed smoothness constraints. Future work will look at using atlas-based fuzzy tissue classification with bias field inhomogeneity correction to improve the tumor probability map.

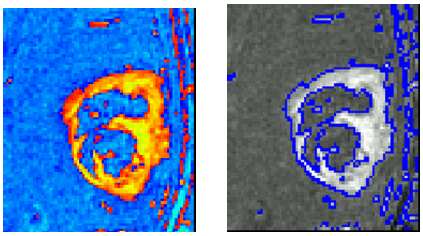

Figure 3. Left: Probability map of tumor vs. non-tumor. Voxels tentatively classified as tumor are in orange; non-tumor in blue. Right: Initialization of the snake.

4.3. Initialization

Many conventional snakes require the user to initialize the snake with a bubble either completely inside or completely outside the object to be segmented. The region competition snake, however, is more robust to variable initialization. We choose the level 0 set of the tumor probability map, where P(tumor)=P(non-tumor), as the initialization. The implicit function is initialized to the distance map of the initial contour, as shown in Figure 3(b). In this way we have a completely automatic initialization of the snake.

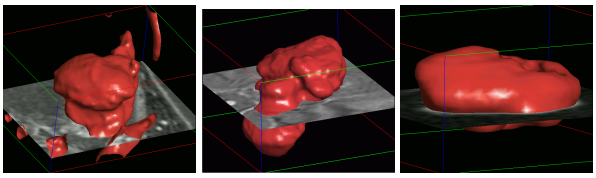

Figure 5. Final segmentations (300 iterations) of other tumor datasets (Tumor022, Tumor025, Tumor026).

4.4. Level-set evolution

Figure 4 shows the implicit function ϕ and the level-set snake at several stages in the segmentation of one tumor dataset. The initialization of the snake corresponds to a simple intensity windowing of the image dataset and shows the difficulty of segmenting tumors with standard morphological operators. After 20 iterations the segmentation is complete, save for some easily removed edge artifacts.

Also shown is the snake after 300 iterations: the balancing force $P(A) - P(B)$ makes the snake very stable; it does not leak into neighboring structures. Classical snakes that use the gradient magnitude as image force often have a tendency to leak through gaps and weak edges.

4.5. Validation

The level-set procedure was successfully run on several tumor datasets, and compared with hand segmentation by an in-house expert rater. The output of each segmentation is a binary image on the same voxel grid as the original MRI. We used the VALMET [1] image segmentation validation framework to examine various metrics of agreement of segmentation. The results for three tumor datasets are shown in Figure 6. The volume overlap measure is a normalized count of voxels in the intersection of two segmentations X and Y, given by $(X \cap Y)/(X \cup Y)$. The Hausdorff distance from X to Y is $max_{x \in X} dist(x, Y)$. Since this is not symmetric, the symmetric Hausdorff metric is the larger of Haus(X,Y) and Haus(Y,X). We also calculate the average distance inside or outside from a point on one surface to the closest point on the other surface.

Dataset	overlap	Haus.	in	out	avg
Tumor020	93.2%	6.92	0.47	1.07	0.59
Tumor022	89.5%	13.02	0.49	4.13	1.49
Tumor025	84.7%	10.73	0.83	1.07	0.85

Figure 6. Comparison with manual segmentation. Surface distances are in voxels.

5. Discussion

We demonstrate a stable, 3D level-set evolution framework applied to automatic segmentation of large blobby-shaped brain tumors in MRIs, using a probability map of tumor versus background to guide the snake propagation.

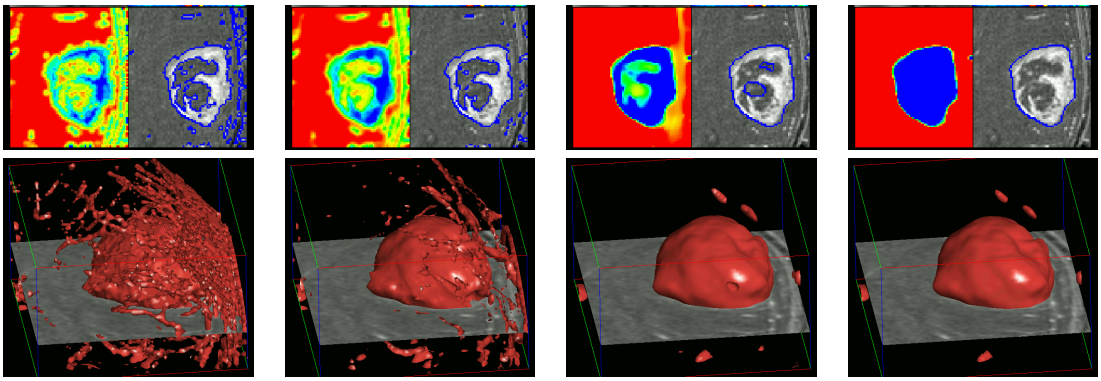

Figure 4. A slice through the implicit function (top) and the level-set snake (bottom) for dataset Tumor020, at initialization, 1 iteration, 20 iterations, and 300 iterations. $c_{\mathrm{MCF}} = 0.7$, $\alpha = 3$, **and** $c_{\mathrm{sm}} = 0.45$

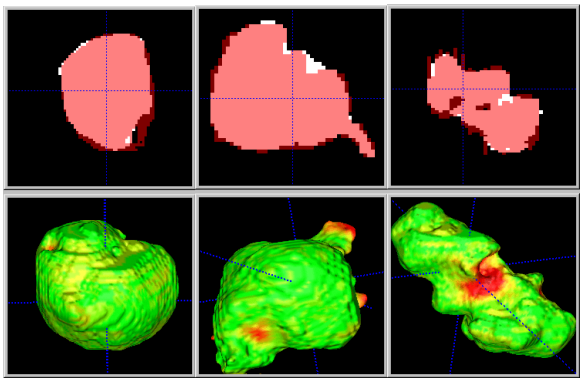

Figure 7. Comparison of automatic procedure with manual segmentation. Top: 2D slice: snake in white, manual in red. Bottom: surface distance, -4 (red) to +4 (blue) voxels. Green is within $\pm$2 voxels. Datasets: Tumor020, Tumor022, Tumor025.

A nonlinear fit of a mixture model to the histogram provides a fuzzy classification map of gadolinium-enhancing voxels, and this probability map is used to guide the propagation of the snake. The snake is very stable, converging in 20-50 iterations and remaining at its solution without "leaking". The snake is also robust to initialization; preliminary tests with various initializations indicate the snake can grow into the entire tumor even when placed over only a small portion of the tumor. The automatic initialization often includes many small spurious regions, such as enhancing blood vessels, however the smoothness constraints on the snake quickly eliminate these from the final segmentation. Preliminary comparisons demonstrate that the automatic segmentation comes close to the manual expert segmentation. Currently, we are validating the snake against repeated segmentations provided by several experts. We are also investigating the sensitivity towards initialization and parameter settings on a larger set of tumor datasets. The level-set evolution algorithm has been packaged in an easy-to-use product, integrated with an interface to manually initialize and clean-up the snake's segmentation.

References

[1] G. Gerig, M. Jomier, and M. Chakos. VALMET: a new validation tool for assessing and improving 3D object segmentation. In W. Niessen and M. Viergever, editors, *MICCAI'01*, volume 2208, pages 516–523, New York, Oct 2001. Springer.

[2] R. Goldenberg, R. Kimmel, E. Rivlin, and M. Rudzsky. Fast geodesic active contours. In *Scale-Space Theories in Computer Vision*, pages 34–45, 1999.

[3] M. Kass, A. Witkin, and D. Terzopoulos. Snakes: Active shape models. *International Journal of Computer Vision*, 1:321–331, 1987.

[4] M. Kaus, S. Warfield, A. Nabavi, E. Chatzidakis, P. Black, J. F.A., and K. R. Segmentation of meningiomas and low grade gliomas in MRI. In C. Taylor and A. Colchester, editors, *MICCAI'99*, volume 1679 of *Lecture Notes in Computer Science*, pages 1–10. Springer, Sept 1999.

[5] M. Leventon, E. Grimson, and O. Faugeras. Statistical shape influence in geodesic active contours. In *CVPR'2000*, 2000.

[6] F. Maes, A. Collignon, D. Vandermeulen, G. Marchal, and P. Suetens. Multi-modality image registration by maximization of mutual information. *IEEE Transactions on Medical Imaging*, 16(2):187–198, Apr 1997.

[7] H. Tek and B. Kimia. Image segmentation by reaction-diffusion bubbles. In *ICCV'95*, pages 156–162, 1995.

[8] H. Tek and B. Kimia. Volumetric segmentation of medical images by three-dimensional bubbles. *Computer Vision and Image Understanding (CVIU)*, 65(2):246–258, 1997.

[9] S. Warfield, J. Dengler, J. Zaers, C. Guttman, W. Wells, G. Ettinger, J. Hiller, and R. Kikinis. Automatic identification of gray matter structures from MRI to improve the segmentation of white matter lesions. *MICCAI'96*, 1(6):326–338, 1996.

[10] S. Warfield, M. Kaus, F. Jolesz, and R. Kikinis. Adaptive template moderated spatially varying statistical classification. In W. M. Wells, A. Colchester, and S. Delp, editors, *MICCAI'98*, volume 1496 of *Lecture Notes in Computer Science*. Springer, Oct 1998.

[11] S. Zhu and A. Yuille. Region competition: Unifying snakes, region growing, and Bayes/MDL for multi-band image segmentation. In *ICCV'95*, pages 416–423, 1995.